Majestic American Journal of Mathematics and Physics
Volume 1, 2026, **pp.** 1-18, **Article ID:** CM2601109003
DOI: 10.65080/majmp.v1.CM2601109003

CONTENT MAJESTIC PUBLISHER

Research Article

A Hybrid Fractional-Order Epidemic Model Incorporating Memory-Dependent Transmission Dynamics

Grienggrai Rajchakit[1], **Maria Malik**[2, *]

[1]*Department of Mathematics, Faculty of Science, Maejo University, Sansai 50290, Chiang Mai, Thailand;*

[2]*Department of Statistics, COMSATS University Islamabad, Pakistan*

Article History
Received: 17 March, 2026 Revised: 05 June, 2026 Accepted: 23 June, 2026 Published: 30 July, 2026

Abstract:

Introduction: This study developed a hybrid fractional-order SEIR model with memory-dependent incidence to examine epidemic transmission under historical exposure effects and intervention-driven regime switching.

Methodology: The model combined Caputo fractional derivatives with admissible convolution kernels, where the kernel mass M_K represents cumulative transmission memory and the fractional order α governs system-level temporal inertia. Analytical results established positivity, boundedness, and well-posedness under non-negative initial conditions and admissible kernel assumptions. The basic reproduction number was derived as: $R_0 = \frac{\sigma\beta M_K}{(\mu+\sigma)(\mu+\gamma)}$, reducing to $R_0 = \frac{\beta M_K}{\gamma}$ in the closed-population case.

Results: This result showed that the epidemic threshold depends on transmission intensity β and kernel properties M_K, whereas the fractional order α mainly influences temporal evolution. Sensitivity analysis showed unit elasticities for β and M_K, inverse sensitivity to recovery rate γ, and limited threshold influence of the latent progression rate in closed populations. The hybrid switching analysis further indicated that intervention regimes should be assessed through regime-specific reproduction numbers and dwell-time conditions.

Conclusion: The framework provided a mathematically grounded extension of classical SEIR models for diseases where delayed infectiousness, environmental persistence, or prolonged memory effects influence epidemic dynamics.

Keywords: Fractional-order models, epidemic modeling, memory-dependent incidence, basic reproduction number, stability analysis, hybrid model.

1. INTRODUCTION

Mathematical models have long served as essential tools for understanding infectious disease transmission and for supporting evidence-based public health decision-making. Classical compartmental frameworks, including the SIR and SEIR models, have been widely employed to describe epidemic dynamics and to identify key thresholds governing disease persistence or elimination [1]. These models are typically formulated using integer-order differential equations, implicitly assuming that the evolution of each epidemiological compartment depends exclusively on its current state [2]. While such assumptions facilitate mathematical analysis and interpretation, they overlook an important feature of real-world epidemics: the influence of historical exposure and cumulative transmission processes.

In many infectious diseases, particularly those characterized by long incubation periods, delayed immune responses, or prolonged infectiousness, the risk of infection cannot be

*Address correspondence to this author at Department of Statistics, COMSATS University Islamabad, Pakistan; E-mail: malik.mariaah@gmail.com

Cite as: G. Rajchakit, M. Malik, " A hybrid fractional-order epidemic model incorporating memory-dependent transmission dynamics," *Majestic American Journal of Mathematics and Physics*, vol. 1, pp. 1-18, article id: CM2601109003, 2026. https://doi.org/10.65080/majmp.v1.CM2601109003

adequately represented as an instantaneous interaction [3]. Instead, it is shaped by past contacts and exposure history accumulated over time. This temporal dependence, commonly referred to as a memory effect, represents a fundamental limitation of integer-order models, which are inherently memoryless and thus unable to capture long-range temporal correlations in disease transmission.

The limitations of memory-free modeling approaches became particularly evident during the COVID-19 pandemic. Forecasts based solely on present-state dynamics often underestimate epidemic persistence, fail to reproduce delayed peaks, and inadequately represented the lagged impact of public health interventions [4]. In many regions, infection levels remained elevated despite stringent control measures, highlighting the need for epidemiological models that explicitly incorporate historical dependence. Fractional-order models have emerged as a natural extension of classical approaches to address this shortcoming. By employing derivatives of non-integer order, fractional calculus intrinsically embeds memory effects into dynamical systems, as the rate of change depends on the entire past trajectory of the system, weighted by a suitable kernel function [5]. This property makes fractional-order formulations particularly well suited for epidemic modeling, where transmission pressure and recovery dynamics often reflect cumulative processes.

The inclusion of memory through fractional derivatives enriches the modeling framework and enables a more faithful representation of epidemic phenomena. For instance, exponential-type kernels describe short-memory processes dominated by recent exposures, whereas power-law kernels account for long-term memory effects in which distant past events continue to influence present dynamics [6]. Such flexibility has proven valuable for capturing prolonged epidemic tails, recurrent waves, and persistent infection patterns observed in real data. However, epidemic transmission is rarely governed by smooth dynamics alone. In practice, disease spread is frequently disrupted by abrupt changes resulting from interventions such as lockdowns, vaccination campaigns, travel restrictions, or behavioral adaptations within populations [7]. These measures induce discontinuous changes in transmission parameters, leading to hybrid dynamics in which multiple regimes of disease spread coexist.

Motivated by these observations, hybrid epidemic models incorporating regime switching have been proposed to represent intervention-driven changes. Meanwhile, fractional-order epidemic models have demonstrated improved performance in fitting real-world data for diseases such as COVID-19 and influenza [8–10]. Empirical studies have shown that fractional formulations more accurately reproduce delayed epidemic peaks, long-tailed decay, and intervention lag effects [11]. Applications to influenza dynamics further suggest that fractional derivatives effectively capture seasonal recurrence and memory embedded in contact networks [12, 13]. Despite these advances, most existing studies have considered either fractional-order models with fixed transmission structures or hybrid integer-order systems without memory. A unified framework combining fractional memory effects with hybrid switching mechanisms remains largely unexplored. Moreover, many studies emphasize numerical simulations while providing limited rigorous analysis. In particular, the explicit influence of memory kernel properties on epidemic thresholds has not been systematically examined, and stability results are often derived heuristically rather than through formal fractional stability theory [14].

This study addresses these gaps by proposing a generalized hybrid fractional-order SEIR model with memory-dependent incidence and regime-switching transmission rates. The model explicitly incorporates admissible memory kernels and demonstrates how their total mass directly influences the basic reproduction number, offering a quantitative characterization of memory effects on epidemic thresholds. Using tools from fractional calculus, including fixed-point arguments and Matignon's stability criterion, the analysis rigorously establishes positivity, boundedness, and well-posedness of solutions. An explicit expression for the basic reproduction number is derived, clarifying its dependence on epidemiological parameters and kernel properties while revealing independence from the fractional order itself.

Beyond threshold analysis, the stability of both disease-free and endemic equilibria is investigated within the fractional-order setting. The results show that the fractional order predominantly affects transient behavior and convergence rates, whereas the memory kernel mass determines whether disease persistence or eradication occurs. The hybrid switching mechanism further enables the model to capture intervention-induced parameter shifts, allowing stability regions to be characterized symbolically and supported by qualitative numerical illustrations. Sensitivity analyses and symbolic–numerical examples demonstrate how memory effects and interventions interact to shape epidemic outcomes.

The contribution of this study is intentionally positioned as an analytical extension rather than a replacement of existing epidemic modeling frameworks. The novelty lies in deriving an explicit reproduction threshold for a memory-dependent fractional SEIR system, showing that the basic reproduction number depends on the total memory-kernel mass M_K, while the fractional order αgoverns transient growth, decay, and persistence patterns. This separation between threshold dynamics and transient dynamics provides a useful interpretive distinction that is often implicit but not clearly formalized in fractional epidemic models. The hybrid switching component further enables intervention regimes to be represented through regime-specific transmission rates and dwell-time assumptions, thereby linking memory-dependent transmission to intervention timing.

This work bridges rigorous mathematical analysis with epidemiological relevance by providing a unified hybrid fractional-order framework for memory-driven epidemics. The

proposed model extends classical epidemic theory and offers insights into the timing and effectiveness of interventions in systems where historical dependence plays a dominant role. The remainder of the paper is organized as follows. Section 2 introduces the necessary mathematical preliminaries. Section 3 presents the formulation of the hybrid fractional-order SEIR model and establishes well-posedness. Section 4 examines positivity, boundedness, and equilibrium structure. Section 5 derives the basic reproduction number, while Section 6 analyzes stability using spectral methods and fractional stability theory. Section 7 provides sensitivity analysis and illustrative examples. Section 8 discusses theoretical implications, policy relevance, and limitations, and Section 9 concludes the paper with a summary and directions for future research.

2. MATHEMATICAL PRELIMINARIES

2.1. Fractional Calculus: Caputo and Riemann–Liouville Derivatives

Fractional calculus generalizes the concept of differentiation and integration from integer orders to arbitrary real or even complex orders. Among several possible definitions, the Caputo and Riemann–Liouville derivatives are the most widely used in modelling physical and biological processes [15]. For a sufficiently smooth function $f(t)$, the Caputo derivative of order $\alpha \in (0,1]$ is defined as (Eq. **2.1**):

$$D_t^{\alpha} f(t) = \frac{1}{\Gamma(1-\alpha)} \int_0^t \frac{f'(\tau)}{(t-\tau)^{\alpha}}\, d\tau, \tag{2.1}$$

where $\Gamma(\cdot)$ is the Euler gamma function [16]. This definition has the advantage of requiring initial conditions in the same form as classical integer-order derivatives, making it particularly suitable for epidemiological modelling. In contrast, the Riemann–Liouville derivative is expressed as:

The Riemann–Liouville derivative of order α, where $n-1 < \alpha < n$, is defined as (Eq. **2.2**):

$${}^{RL}D_t^{\alpha} f(t) = \frac{1}{\Gamma(n-\alpha)} \frac{d^n}{dt^n} \int_0^t (t-\tau)^{n-\alpha-1} f(\tau)\, d\tau. \tag{2.2}$$

Unlike the Caputo derivative, the Riemann–Liouville formulation often leads to initial conditions expressed in terms of fractional integrals, which are less direct for epidemiological interpretation. The Laplace transform expressions are valid for functions of exponential order whose Caputo derivatives and convolution integrals exist on the considered time interval.

which often leads to initial conditions expressed in fractional integrals, a feature that complicates biological interpretation [17]. The Caputo definition is therefore preferred in the current study, as it allows us to specify initial numbers of susceptible, exposed, infected, and recovered individuals, consistent with epidemiological practice.

The key feature of both derivatives is their non-locality. Unlike integer-order differentiation, where the derivative at a point depends solely on local behavior, fractional derivatives depend on the entire history of the function. This historical dependence introduces memory into the system, which is central to the motivation of this research.

2.2. Convolution Operators and Memory Kernels

The non-local property of fractional derivatives can be formally expressed through convolution operators. Let $K_{\vartheta}(t)$ be a non-negative kernel function parameterized by ϑ. The convolution of K_{ϑ} with a function $I(t)$ is given by (Eq. **2.3**):

$$(K_{\vartheta} * I)(t) = \int_0^t K_{\vartheta}(t-\tau) I(\tau) d\tau\,. \tag{2.3}$$

In epidemic models, this convolution plays the role of memory-dependent incidence, as it weights past infectious individuals by the memory kernel. The total mass of the kernel, defined as (Eq. **2.4**):

$$M_K = \int_0^{\infty} K_{\vartheta}(s) ds\,, \tag{2.4}$$

quantifies the cumulative influence of past infections. Although kernel mass summarizes cumulative historical infectiousness, it should not be interpreted as identical to all memory effects. Its direct mathematical role is to scale the integrated transmission contribution and therefore influence the reproduction threshold. In contrast, the kernel shape determines temporal characteristics such as peak timing, persistence, and decay behavior. The interpretation of M_K depends on the kernel family. For an exponential kernel, the mass is finite and reflects short-term memory with rapid decay, while a power-law kernel yields heavier tails, indicating long-lasting memory where even distant past exposures affect current transmission. This flexibility enables models to capture fast-decaying and persistent memory effects, aligning the mathematics more closely with observed epidemiological data.

Admissible kernels in fractional epidemic models include exponential functions of the form $K_{\vartheta}(s) = \lambda e^{-\lambda s}$, power-law kernels $K_{\vartheta}(s) = \frac{s^{-\vartheta}}{\Gamma(1-\vartheta)}$, and Mittag–Leffler kernels that interpolate between exponential and power-law behaviours. Each family corresponds to a different epidemiological interpretation. Exponential kernels approximate diseases where recent contacts dominate infection probability [18], while power-law kernels describe diseases with long incubation periods or recurrent exposures [19]. The Mittag–Leffler kernel provides a flexible framework for capturing both intermediate and complex memory behaviors, making it particularly relevant for hybrid fractional models [14].

2.3. Laplace Transform Properties and Analytical Tools

Fractional calculus analysis often relies on the Laplace transform, as it provides tractable forms for both Caputo derivatives and convolution operators. The Laplace transform of the Caputo derivative of a function $f(t)$ with initial condition $f(0) = f_0$ is (Eq. **2.5**):

$$\mathcal{L}\{D_t^{\alpha} f(t)\}(s) = s^{\alpha} \hat{f}(s) - s^{\alpha} - 1 f_0, \tag{2.5}$$

where $\hat{f}(s)$ denotes the Laplace transform of $f(t)$ [20]. This relationship enables the transformation of fractional differential

equations into algebraic equations in the Laplace domain, which are often more amenable to stability and spectral analysis.

Another essential tool is the convolution theorem, which states that the Laplace transform of a convolution is simply the product of the Laplace transforms of its components. For a kernel K_ϑ and an incidence function $I(t)$, (Eq. **2.6**):

$$\mathcal{L}\{(K_\vartheta * I)(t)\}(s) = \widehat{K_\vartheta}(s) \cdot \hat{I}(s). \tag{2.6}$$

This property simplifies the analysis of memory-incidence terms and allows explicit dependence of system stability on the kernel mass and its spectral properties. In addition, Grönwall-type inequalities for fractional systems are frequently employed to establish bounds on solutions and to prove positivity and boundedness [21].

2.4. Stability Criteria in Fractional Systems

The analysis of stability in fractional-order systems requires specialized tools because the classical criteria used in integer-order systems do not directly apply. A key result is Matignon's theorem, which provides a criterion for the asymptotic stability of linear fractional-order systems [22]. According to this theorem, consider a linear system $D_t^\alpha x(t) = Ax(t)$ with $\alpha \in (0,1]$. The system is asymptotically stable if and only if the eigenvalues λ of the matrix A satisfy (Eq. **2.7**):

$$|\arg(\lambda)| > \frac{\alpha\pi}{2}. \tag{2.7}$$

This criterion highlights the effect of fractional order on stability regions. Unlike integer-order systems, where stability depends on whether eigenvalues lie in the left half-plane, fractional systems require eigenvalues to lie outside a sector whose angle depends on α. This dependence reveals how memory effects influence the resilience of equilibrium states, making fractional stability analysis more nuanced than classical methods.

2.5. Functional Spaces and Well-Posedness

A rigorous analysis of fractional-order epidemic models necessitates the precise specification of the functional spaces in which solutions are defined. Typically, solutions are sought in appropriate Banach spaces of continuous or integrable functions over non-negative time intervals, where the associated norms are designed to capture the inherent nonlocality of fractional differential operators. The existence and uniqueness of solutions are commonly established by applying fixed-point techniques, most notably Banach's contraction principle, within these functional settings [23].

Moreover, ensuring the epidemiological validity of the model requires that all state variables remain biologically meaningful throughout the evolution process. In particular, the non-negativity and boundedness of the susceptible, exposed, infectious, and recovered populations must be rigorously guaranteed. By employing fractional comparison principles together with suitably chosen admissible kernels, it can be shown that the model solutions remain confined to a positively invariant and bounded region for all time. These mathematical properties are not only essential from a theoretical standpoint but also fundamental for preserving the biological interpretability and reliability of the proposed epidemic model.

2.6. Kernel Families and Epidemiological Interpretation

Different classes of memory kernels influence not only the analytical behavior of fractional-order epidemic systems but also their epidemiological interpretation. Exponential-type kernels, characterized by a finite memory mass, are well-suited for modeling diseases such as seasonal influenza, where transmission dynamics are primarily governed by recent exposure events [24]. In contrast, power-law kernels with heavy tails are capable of capturing long-term memory and persistence effects, which are particularly relevant for diseases with complex immune responses, such as tuberculosis or viral infections exhibiting prolonged latency periods. Mittag–Leffler kernels provide an intermediate description between these two extremes, allowing for a gradual decay of memory and accommodating more intricate temporal dependencies observed in real-world epidemiological data.

The ability to flexibly select the kernel function within the fractional-order framework constitutes a major advantage of this modeling approach. It enables the formulation of disease-specific models that faithfully represent diverse memory mechanisms while preserving analytical tractability and mathematical generality.

3. MODEL FORMULATION

3.1. Compartmental Design

The proposed framework is built upon a classical compartmental structure that partitions the total population into four mutually exclusive classes: susceptible $S(t)$, exposed $E(t)$, infectious $I(t)$, and recovered $R(t)$. This SEIR configuration is particularly appropriate for infectious diseases characterized by a non-negligible incubation period, during which individuals are infected but not yet capable of transmitting the disease. Throughout the considered time horizon, the total population is assumed to remain constant, implying that births and natural deaths are either balanced or negligible relative to disease-driven dynamics. Although this assumption simplifies the model formulation, it is standard in mathematical epidemiology, especially when the primary objective is to isolate and analyze the impact of memory effects on transmission processes rather than demographic variations. Extensions incorporating vital dynamics can be accommodated within the proposed framework; however, such additions would complicate the analysis without fundamentally altering the core mathematical insights related to memory-dependent transmission [25]. This fractional formulation inherently incorporates memory effects, ensuring that the rates of new infections, disease progression, and recovery at time $t$depend not only on the current state of the system but also on the cumulative history of the epidemic up to time t.

The use of both Caputo fractional derivatives and an explicit convolution kernel do not imply a duplication of the same memory mechanism. In the proposed framework, the Caputo derivative represents system-level memory, meaning that the

rates of change of epidemiological compartments depend on the past trajectory of the state variables. This captures inertia in disease progression, recovery, and relaxation toward equilibrium. By contrast, the convolution kernel $K_\vartheta$represents transmission-specific memory, meaning that present infection pressure depends on the weighted history of infectious individuals. Epidemiologically, this may reflect delayed infectiousness, environmental persistence, repeated exposure, or reporting delay. Thus, αcontrols the temporal response of the compartmental system, whereas K_ϑ and its mass M_K control the accumulated force of infection. This distinction explains why $M_K$enters the reproduction threshold, while αprimarily affects transient dynamics.

3.2. Memory-Dependent Incidence

The key novelty of the present model lies in the formulation of incidence, that is, the rate at which susceptible individuals become exposed due to contact with infectious individuals. In classical models, the incidence is typically given by $\beta S(t)I(t)$, where β denotes the transmission coefficient. This formulation assumes that the force of infection depends solely on the current number of infectious individuals. In contrast, the proposed model incorporates memory by defining the incidence function as a convolution of the infectious population with a kernel K_ϑ. Specifically, the infection pressure at the time t is given by (Eq. **3.1**):

$$\Lambda(t) = \beta N S(t) \int_0^t K_\vartheta(t-\tau) I(\tau) d\tau, \tag{3.1}$$

Where, N is the total population, and K_ϑ represents an admissible memory kernel that weights past infections. The biological interpretation is that the infection risk faced by susceptible individuals is not simply proportional to the number of currently infectious persons but instead reflects a weighted accumulation of all individuals who were infectious in the past, with the weighting determined by the kernel.

This formulation captures a wide range of epidemiological realities. For example, in diseases where recent exposure dominates, an exponential kernel ensures that the influence of past infections decays rapidly. Conversely, in diseases where prolonged contact or environmental persistence of pathogens is relevant, a power-law kernel reflects the enduring effect of older infections [26]. The inclusion of kernel mass M_K provides a measure of the cumulative influence of past exposures on present dynamics and plays a crucial role in determining the reproduction number and stability conditions.

For consistency, the notation used throughout the paper is fixed as follows. The parameter σdenotes only the biological progression rate from the exposed class to the infectious class. The switching signal is denoted by $q(t)$, not by σ. The transmission rate under regime j is denoted by β_j, while the time-varying transmission rate is denoted by $\beta(t) = \beta_{q(t)}$. Thus, when the system operates in regime j, the corresponding reproduction number is written as $R_0^{(j)}$. This notation is used consistently in the model equations, stability analysis and sensitivity discussion.

The hybrid structure is described through a switching signal $q(t)$. Let $q(t): [0,\infty) \to \mathcal{J} = \{1,2,\dots,m\}$, where $q(t) = j$ indicates that the epidemic system is operating under an intervention regime j. Each regime is associated with a transmission coefficient $\beta_j > 0$, so that the time-dependent transmission rate is written as $\beta(t) = \beta_{q(t)}$. The symbol $\sigma > 0$is reserved exclusively for the exposed-to-infectious progression rate and is not used to denote switching. The dwell time of a regime is the duration for which $q(t) = j$remains active before switching to another regime. Accordingly, all regime-specific threshold quantities are written as $R_0^{(j)}$, computed using β_j.

3.3. Hybrid Fractional Formulation

While fractional-order derivatives and convolution kernels embed memory into the epidemic system, real-world disease spread is also subject to abrupt changes arising from interventions. Public health measures such as lockdowns, social distancing mandates, vaccination campaigns, or behavioral changes in the population effectively alter the transmission rate over time [27]. To capture this feature, the present model allows the transmission coefficient $\beta(t)$ to vary in a piecewise constant manner, representing different regimes of disease spread. For example, a high value of β may correspond to periods of unrestricted contact, while a lower value corresponds to phases when strict measures are enforced.

This hybrid formulation combines two dimensions of realism: fractional-order derivatives for memory effects and hybrid switching structures for intervention-induced dynamics. Formally, the state equations are expressed as (Eq. **3.2**, **3.3**, **3.4**, **3.5**):

$$D_t^\alpha S(t) = -\Lambda(t), \tag{3.2}$$

$$D_t^\alpha E(t) = \Lambda(t) - \sigma E(t), \tag{3.3}$$

$$D_t^\alpha I(t) = \sigma E(t) - \gamma I(t), \tag{3.4}$$

$$D_t^\alpha R(t) = \gamma I(t), \tag{3.5}$$

where σ represents the rate at which exposed individuals become infectious, and γ is the recovery rate. The incidence $\Lambda(t)$ is defined as above, incorporating both the fractional structure and the kernel convolution. The inclusion of $\beta(t)$ as a piecewise-constant function introduces hybrid behavior into the system and represents sudden changes in transmission conditions caused by interventions, policy shifts, or population-level behavioural responses.

3.4. Conditions for Well-Posedness

A critical requirement for any epidemic model is that it be biologically and mathematically well-posed. This means that solutions should exist, be unique, and remain within epidemiologically meaningful bounds forever. In the present context, this translates into three conditions: positivity, boundedness, and admissibility of kernels.

Positivity ensures that population compartments cannot assume negative values, which would be biologically

meaningless. This property can be established using fractional comparison principles, which extend classical comparison results to fractional differential equations. These principles guarantee that if initial conditions are non-negative, the solutions remain non-negative for all subsequent times.

Boundedness requires that the total population not grow unboundedly. Since the system is closed and no new individuals are introduced beyond the initial total population, construction satisfies boundedness. However, the rigorous proof employs Grönwall-type inequalities adapted to fractional systems, which show that the sum $S(t) + E(t) + I(t) + R(t) = N$ is preserved under the dynamics.

The admissibility of kernels requires that K_ϑ is non-negative, integrable, and possesses a finite or controlled mass M_K. These properties ensure that the memory-incidence term is mathematically well-defined and biologically interpretable. In particular, the integrability of K_ϑ guarantees that the convolution $\int_0^t K_\vartheta(t-\tau)I(\tau)d\tau$ is finite for bounded $I(t)$. The choice of admissible kernels is thus central to establishing the well-posedness of the model.

3.5. Interpretation and Relevance

The proposed formulation extends the classical SEIR framework in two fundamental directions. First, it introduces fractional-order dynamics, thereby embedding memory effects directly into the epidemic evolution equations. This formulation reflects the realistic observation that infection and recovery processes are influenced not only by the current epidemiological state but also by accumulated past exposures. Second, the model incorporates hybrid regime switching to capture the discontinuous and policy-driven nature of real-world public health interventions. Together, these features yield a flexible and realistic modeling framework that surpasses the descriptive capabilities of both conventional integer-order models and fractional-order models lacking regime-switching mechanisms.

From a theoretical perspective, the model provides a systematic platform for examining the interaction between memory effects and intervention strategies in determining epidemic thresholds, stability properties, and long-term behavior. From an applied standpoint, it offers insights into how public health policies may interact with intrinsic memory mechanisms in disease transmission, thereby modulating intervention effectiveness. For instance, the introduction of a lockdown during periods when the memory kernel exhibits substantial cumulative mass, indicating strong persistence of past infections, may lead to markedly different epidemic outcomes than an intervention implemented under weaker memory conditions. Such observations underscore the importance of accounting for memory effects when designing timely and effective epidemic control strategies. To clarify the computational and analytical sequence of the proposed hybrid fractional-order memory-dependent SEIR framework, Fig. (**1**) presents the stepwise workflow of the model. The algorithm begins with the input of epidemiological parameters and the selection of an admissible memory kernel. The kernel mass $M_K$is then computed to quantify cumulative transmission memory. Next, the hybrid switching signal is defined to represent intervention regimes, followed by the construction of the memory-dependent incidence function. The fractional SEIR system is then solved numerically, and regime-specific reproduction numbers are calculated. Finally, stability conditions, sensitivity analysis, and epidemiological outputs are generated.

As shown in Fig. (**1**), the proposed framework links kernel selection, hybrid switching, fractional numerical solution, reproduction-number computation, stability assessment, and sensitivity analysis within a single structured workflow.

3.6. Computational Complexity of the Proposed Algorithm

The computational cost of the proposed hybrid fractional memory-dependent SEIR algorithm is mainly determined by the evaluation of the fractional derivative and the convolution-based memory incidence. Let $n$denote the number of time steps, $m$the number of switching regimes, and $d = 4$ the number of epidemiological compartments. In a direct time-stepping implementation, the Caputo fractional derivative requires storing and summing historical state values, which gives a computational cost of $O(dn^2)$over the full simulation horizon. Similarly, direct evaluation of the convolution term $(K_\vartheta * I)(t)$ at each time step requires summation over all previous infectious states, resulting in $O(n^2)$ time complexity and $O(n)$ memory complexity.

The hybrid switching component introduces only a minor additional cost. If the switching signal $q(t)$ is pre-defined, determining the active transmission regime at each time step requires $O(n)$operations. Therefore, the overall direct implementation has time complexity $O(n^2 + mn)$, which is dominated by the fractional-memory and convolution calculations. Since $m \ll n$in most epidemic simulations, the effective complexity is $O(n^2)$. The memory requirement is $O(dn + n)$, which simplifies to $O(n)$.

For exponential kernels, the convolution can be updated recursively, reducing the convolution cost from $O(n^2)$to $O(n)$. For general kernels, fast convolution methods based on FFT or sum-of-exponentials approximation may reduce the cost to approximately $O(n \log n)$ or near-linear complexity. Therefore, the proposed algorithm is computationally feasible for moderate epidemic time horizons, but long-horizon simulations with heavy-tailed kernels may require accelerated memory approximation techniques.

4. ANALYTICAL PROPERTIES

4.1. Positivity and Biological Feasibility

A fundamental requirement of any epidemic model is that its solutions remain biologically meaningful. In particular, the compartments representing susceptible, exposed, infectious, and recovered individuals must remain non-negative for all time. Negative compartment values violate biological feasibility; therefore, positivity preservation is a fundamental mathematical requirement in compartmental epidemic models. This property is established through comparison principles adapted to fractional differential equations in the hybrid fractional-order framework.

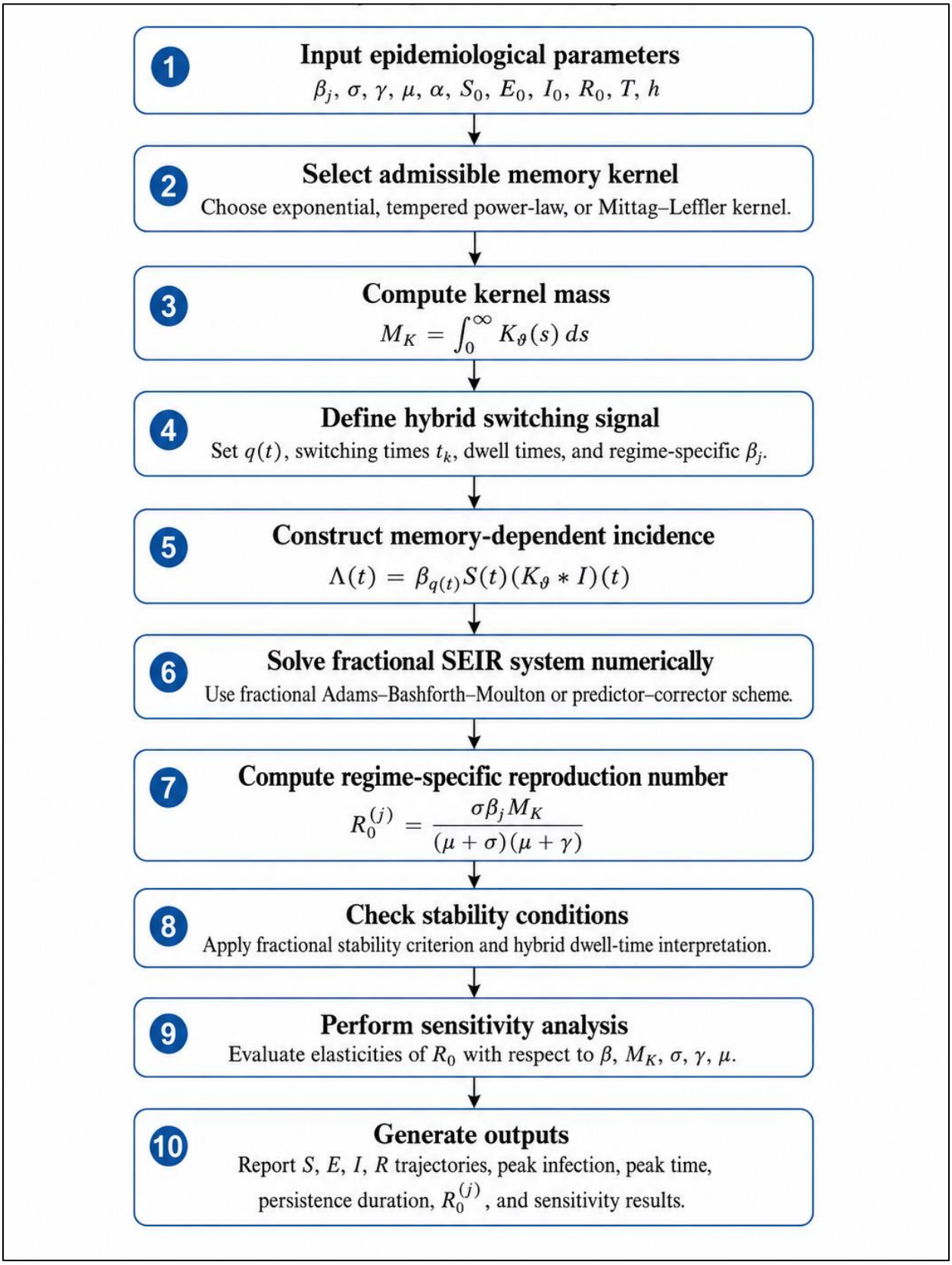

Fig. (1). Stepwise flowchart of the proposed hybrid fractional-order memory-dependent SEIR algorithm.

Consider the system formulated in Section 3, with initial conditions $S(0) \geq 0$, $E(0) \geq 0$, $I(0) \geq 0$, and $R(0) \geq 0$. The right-hand sides of the differential equations are non-negative whenever the compartments are non-negative, except for the susceptible equation, where the derivative is non-positive. This ensures that susceptible individuals decrease but never become negative. The fractional comparison principle guarantees that if the initial state is non-negative, then the trajectory remains confined to the non-negative orthant of $\mathbb{R}^4$.

To illustrate, the derivative of $S(t)$ satisfies (Eq. **4.1**):

$$D_t^{\alpha} S(t) = -\Lambda(t) \leq 0, \tag{4.1}$$

which implies that $S(t)$ is monotonically decreasing but bounded below by zero. Similarly, the derivative of $E(t)$ satisfies (Eq. **4.2**):

$$D_t^{\alpha} E(t) = \Lambda(t) - \sigma E(t), \tag{4.2}$$

where $\Lambda(t) \geq 0$ represents the non-negative memory-dependent infection pressure. Thus, when $E(t) = 0$, the exposed compartment cannot cross into negative values because the inflow term remains non-negative and the outflow term vanishes.

4.2. Boundedness and Population Conservation

In addition to positivity, it is essential to demonstrate that the solutions remain bounded within the total population. The system's boundedness follows from the population conservation, since no births or natural deaths are considered in the current formulation. Let $N(t) = S(t) + E(t) + I(t) + R(t)$. Adding the four equations of the system gives: (Eq. **4.3**):

$$D_t^{\alpha} N(t) = D_t^{\alpha} S(t) + D_t^{\alpha} E(t) + D_t^{\alpha} I(t) + D_t^{\alpha} R(t) = 0. \tag{4.3}$$

This implies that $N(t)$ remains constant in time, equal to the initial population $N(0)$. Thus, the feasible region for the system is the simplex (Eq. **4.4**):

$$\Omega = \{(S, E, I, R) \in \mathbb{R}_+^4 : S + E + I + R = N(0)\} \tag{4.4}$$

The boundedness of the model is therefore guaranteed by construction: each compartment remains between zero and the total population, while their sum is invariant. This result is mathematically rigorous and critical for ensuring epidemiological realism, as populations cannot grow unboundedly in a closed system.

4.3. Existence and Uniqueness of Solutions

Let $X_T = C([0, T], \Omega)$ denote the Banach space of continuous vector-valued functions defined on $[0, T]$ with values in the feasible region Ω [28]. This space is equipped with the supremum norm (Eq. **4.5**):

$$\| x \|_{\infty} = \sup_{t \in [0,T]} \| x(t) \| \tag{4.5}$$

The Caputo fractional-order system can be rewritten as the equivalent Volterra integral equation (Eq. **4.6**):

$$(\mathcal{T}x)(t) = x_0 + \frac{1}{\Gamma(\alpha)} \int_0^t (t - s)^{\alpha - 1} F(s, x(s))\, ds \tag{4.6}$$

where F denotes the full vector field of the hybrid fractional SEIR system and $\mathcal{T}$ is the associated integral operator. Assume that F is Lipschitz continuous on the feasible region Ω. Since the incidence term contains the convolution $k * I$, the admissibility of the kernel gives (Eq. **4.7**):

$$\| k * (I_1 - I_2) \|_{\infty} \leq M_k \| I_1 - I_2 \|_{\infty} \tag{4.7}$$

Where,

$$M_k = \int_0^{\infty} k(s)\, ds$$

is the total mass of the memory kernel. Hence, the memory-dependent incidence term remains bounded and Lipschitz on Ω. Let $L_{\Omega} > 0$ denote the resulting Lipschitz constant of the full vector field on Ω, including the contribution of the convolution term.

For any $x, y \in X_T$, the induced operator estimate is

$$\| \mathcal{T}x - \mathcal{T}y \|_{\infty} \leq \frac{L_{\Omega}}{\Gamma(\alpha)} \sup_{t \in [0,T]} \int_0^t (t - s)^{\alpha - 1} \| x(s) - y(s) \|\, ds$$

Using the supremum norm, this becomes, (Eq. **4.8**):

$$\| \mathcal{T}x - \mathcal{T}y \|_{\infty} \leq \frac{L_{\Omega} T^{\alpha}}{\Gamma(\alpha + 1)} \| x - y \|_{\infty} \tag{4.8}$$

Define the contraction coefficient,

$$q = \frac{L_{\Omega} T^{\alpha}}{\Gamma(\alpha + 1)}$$

Therefore, $\mathcal{T}$ is a contraction whenever, (Eq. **4.9**):

$$q < 1, \text{ or equivalently } T < \left(\frac{\Gamma(\alpha + 1)}{L_{\Omega}} \right)^{1/\alpha} \tag{4.9}$$

Under condition (Eq. **4.9**), Banach's fixed-point theorem guarantees a unique local solution on [0, T]. For longer time intervals, the solution can be extended stepwise over subintervals satisfying the same contraction condition. Since positivity and boundedness keep the solution inside the invariant feasible region Ω, the local solution can be continued globally. Thus, the proposed hybrid fractional SEIR system is well posed under non-negative initial conditions and admissible kernel assumptions [29, 30].

4.4. Disease-Free Equilibrium

The Disease-Free Equilibrium (DFE) represents the state where the infection is absent, and the population consists entirely of susceptible individuals. In the present model, the DFE is given by (Eq. **4.10**):

$$E_0 = (S^*, E^*, I^*, R^*) = (N, 0, 0, 0) \tag{4.10}$$

At this equilibrium, the incidence $\Lambda(t)$ vanishes since there are no infectious individuals to sustain transmission. The

stability of this equilibrium, which will be discussed in Section 6, is determined by the basic reproduction number R_0. If $R_0 < 1$, the DFE is stable, meaning that small perturbations, such as the introduction of a few infected individuals, will not lead to an outbreak. Conversely, if $R_0 > 1$, the DFE becomes unstable and the epidemic may persist.

The derivation of the DFE within the fractional and hybrid framework confirms that memory and switching do not eliminate the classical epidemic threshold phenomenon, though they do modify the conditions under which it occurs. This reflects the robustness of the threshold concept across modelling frameworks.

4.5. Endemic Equilibrium

In addition to the disease-free equilibrium, the model may admit an endemic equilibrium E^*, where infection persists at a positive level. At this steady state, the infection subsystem satisfies the following balance conditions (Eq. **4.11**):

$$\Lambda^* = \sigma E^*, \quad \sigma E^* = \gamma I^*, \quad I^* > 0 \tag{4.11}$$

These relations show that, at equilibrium, the rate at which susceptible individuals enter the exposed class is balanced by the progression rate from the exposed class to the infectious class, while the infectious class is balanced by recovery. Substituting these equilibrium balance relations into the memory-dependent incidence definition yields endemic-state quantities expressed in terms of the transmission rate, exposed-to-infectious progression rate, recovery rate, and kernel mass M_k.

The feasibility of the endemic equilibrium requires all epidemiological compartments to remain positive and is governed by the threshold condition $R_0 > 1$. When this condition holds under the stated admissibility assumptions, a biologically meaningful endemic equilibrium may exist. Conversely, when $R_0 \leq 1$, the infection cannot sustain itself and the disease-free equilibrium remains the relevant long-term state. The stability of the endemic equilibrium is examined later through the corresponding linearized system and fractional-sector stability conditions.

5. BASIC REPRODUCTION NUMBER R_0

5.1. Linearization At the Disease-Free Equilibrium

We derive R_0 for the hybrid fractional SEIR model with memory-dependent incidence by linearizing the infection subsystem around the disease-free equilibrium (DFE). As in Section 3, let $S(t), E(t), I(t), R(t)$ denote the compartment sizes and let the incidence be (Eq. **5.1**):

$$\Lambda(t) = \beta S(t) \int_0^t K_\vartheta(t-\tau) I(\tau) d\tau, \tag{5.1}$$

with an admissible kernel K_ϑ of mass $M_K = \int_0^\infty K_\vartheta(s)\, ds$. For notational clarity in the derivation, it is convenient to work with normalized fractions $s = \frac{S}{N}, e = \frac{E}{N}, i = \frac{I}{N}, r = \frac{R}{N}$ so that $s + e + i + r = 1$, and to absorb any constant N into β when needed. Hybrid switching of $\beta(t)$ is present in the full model, but R_0 is defined per constant regime, so we begin with $\beta(t) \equiv \beta$ in a fixed phase. The infected subsystem (e, i) near the DFE $(s^*, e^*, i^*, r^*) = (1,0,0,0)$ is then (Eq. **5.2**, **5.3**):

$$D_t^\alpha e(t) = \beta \int_0^t K_\vartheta(t-\tau) i(\tau) d\tau - (\mu + \sigma) e(t), \tag{5.2}$$

$$D_t^\alpha i(t) = \sigma e(t) - (\mu + \gamma) i(t), \tag{5.3}$$

where σ is the progression rate from exposed to infectious, γ is the removal or recovery rate from infectious, and μ is an optional natural removal rate. Sections 3 and 4 analysed the closed population case with $\mu = 0$; we include μ here to present the general formula and later specialize in $\mu = 0$.

5.2. Laplace-Domain Derivation and The Threshold Equation

The next-generation threshold can be obtained cleanly in the Laplace domain. Take Laplace transforms of the linearized system with zero initial conditions, which is appropriate when computing the response to an infinitesimal introduction of infection at the DFE. Using $\hat{f}(s) = \mathcal{L}\{f(t)\}(s)$ and $\mathcal{L}\{D_t^\alpha f\}(s) = s^\alpha \hat{f}(s)$ for zero initial data, and writing $\widehat{K_\vartheta}(s) = \mathcal{L}\{K_\vartheta\}(s)$, we obtain (Eq. **5.4**, **5.5**, **5.6**):

$$s^\alpha \hat{e}(s) = \beta \widehat{K_\vartheta}(s) \hat{\imath}(s) - (\mu + \sigma) \hat{e}(s), \tag{5.4}$$

$$s^\alpha \hat{\imath}(s) = \sigma \hat{e}(s) - (\mu + \gamma) \hat{\imath}(s). \tag{5.5}$$

Eliminating $\hat{e}(s)$ gives

$$(s^\alpha + \mu + \gamma)(s^\alpha + \mu + \sigma) \hat{\imath}(s) = \sigma \beta \widehat{K_\vartheta}(s) \hat{\imath}(s). \tag{5.6}$$

A nontrivial solution requires the characteristic equation (Eq. **5.7**):

$$(s^\alpha + \mu + \gamma)(s^\alpha + \mu + \sigma) = \sigma \beta \widehat{K_\vartheta}(s). \tag{5.7}$$

The early growth or decay of small perturbations is governed by roots s with $\Re(s) > 0$ when the right side is large, or $\Re(s) < 0$ when it is small. The reproduction threshold is identified at the point where the dominant root crosses the imaginary axis. Evaluating at $s = 0$ exploits $\widehat{K_\vartheta}(0) = \int_0^\infty K_\vartheta(s)\, ds = M_K$ and yields the threshold condition (Eq. **5.8**):

$$(\mu + \gamma)(\mu + \sigma) = \sigma \beta M_K. \tag{5.8}$$

Define as (Eq. **5.9a**):

$$R_0 = \frac{\sigma \beta M_K}{(\mu+\sigma)(\mu+\gamma)}. \tag{5.9a}$$

The resulting reproduction number shows that the epidemic threshold is governed by the combined effect of transmission intensity, cumulative memory and removal processes. In the closed-population case, the expression reduces to (Eq. **5.9b**):

$$R_0 = \frac{\beta M_K}{\gamma} \tag{5.9b}$$

This formula recovers the classical SEIR threshold when $M_K = 1$. The fractional order α influences trajectory-level characteristics while remaining absent from the threshold expression. Thus, the kernel mass M_K controls threshold amplification, whereas αcontrols temporal inertia.

5.3. Interpretation Through The Next-Generation Operator

The same formula arises from an intuitive next-generation argument that clarifies the epidemiological meaning of each factor. Consider a single newly infected individual entering the exposed compartment at time zero in a fully susceptible population. The probability that this individual progresses from E to I rather than being removed naturally is $\frac{\sigma}{\mu+\sigma}$. Conditional on entering I, the expected time spent infectious before removal is $\frac{1}{\mu+\gamma}$. During the time in I, the instantaneous force of infection applied to the susceptible is $\beta\,(K_\vartheta * i)(t)$. Integrating over time and invoking the convolution identity $\int_0^\infty (K_\vartheta * i)(t)\,dt = M_K \int_0^\infty i(t)\,dt$ leads to an expected total infectious "weight" equal to M_K times the area under the infectious trajectory. Multiplying these factors yields (Eq. **5.10**):

$$R_0 = \beta \times M_K \times \frac{\sigma}{\mu+\sigma} \times \frac{1}{\mu+\gamma}, \tag{5.10}$$

which matches the Laplace-domain result. This decomposition shows that R_0 is the product of a contact-transmission factor β, a memory amplification factor M_K, a progression probability $\frac{\sigma}{\mu+\sigma}$, and a mean infectious residency $\frac{1}{\mu+\gamma}$. The fractional order α governs how quickly these events unfold in time, but does not change their probabilities and expected totals at the linear threshold, which explains its absence from R_0.

5.4. Specialization, Limiting Cases, and Hybrid Regimes

In the closed population case analyzed in Sections 3 and 4, set $\mu = 0$. The formula reduces to (Eq. **5.11**):

$$R_0 = \frac{\beta M_K}{\gamma}, \tag{5.11}$$

which is the classical SEIR threshold scaled by the kernel mass. The latent rate σ drops out because, in the absence of natural attrition in the exposed state, all exposed individuals ultimately progress to infectious and contribute the same expected infectious time $\frac{1}{\gamma}$; σ changes the generation timing but not the count of secondary infections at the threshold. If the kernel is exponential $K_\vartheta(s) = \lambda e^{-\lambda s}$, then $M_K = 1$ and memory does not alter R_0; in this case, memory affects only the temporal filtering of incidence. For heavy-tailed families such as power-law or Mittag–Leffler kernels with finite mass, $M_K > 1$ effectively inflates the threshold by increasing the integrated weight of past infectiousness. This captures the intuitive idea that persistent memory in transmission amplifies the cumulative opportunity for new infections.

Hybrid switching of $\beta(t)$ across regimes $\{\beta_j\}$ produces regime-specific reproduction numbers (Eq. **5.12**):

$$R_0^{(j)} = \frac{\sigma \beta_j M_K}{(\mu+.\sigma)(\mu+\gamma)}. \tag{5.12}$$

These regime values are the natural quantities to report for interventions that change contact intensity in discrete phases. They serve as inputs to the stability analysis under switching in Section 6, where the combined effect of alternating regimes is assessed using fractional stability tools. In particular, the DFE can remain stable even if some phases have $R_0^{(j)} > 1$, providing the overall switching pattern and dwell times places the linearized spectrum in the appropriate fractional stability sector.

5.5. Relation to Initial Growth and to The Fractional Order

The reproduction number for the proposed memory-dependent fractional SEIR system is (Eq. **5.13**):

$$R_0 = \frac{\sigma \beta M_K}{(\mu+\sigma)(\mu+\gamma)}, \tag{5.13}$$

The threshold expression in Eq. (**5.13**) provides the reproduction criterion used in the stability analysis that follows. Initial growth or decay is determined by the roots of the Laplace-domain characteristic equation, while trajectory-level features such as peak timing and relaxation speed are assessed through the fractional response of the system. Thus, (Eq. **5.13**) is used as the threshold condition, whereas the characteristic equation provides the basis for interpreting early epidemic kinetics.

5.6. Summary and Implications

The basic reproduction number for the hybrid fractional SEIR model with memory-dependent incidence is (Eq. **5.14**):

$$R_0 = \frac{\sigma \beta M_K}{(\mu+\sigma)(\mu+\gamma)} \quad (general\ case),\ R_0 = \frac{\beta M_K}{\gamma} \quad (closed\ population,\ \mu = 0). \tag{5.14}$$

It is determined by a contact-memory factor βM_K divided by the product of removal rates in the exposed and infectious stages, with a progression factor σ when $\mu > 0$. The fractional order α primarily influences transient kinetics around the threshold. This separation is useful for analysis and for policy interpretation. Memory acts as a transparent multiplier through M_K, so comparing two admissible kernel families amounts to comparing their masses, while their shapes are reflected in transient observables rather than in the threshold. These observations will be carried into Section 6, where the stability of both DFE and endemic equilibria is established in the fractional setting and extended to the hybrid switching case.

6. STABILITY ANALYSIS

6.1. Local Stability of The Disease-Free Equilibrium

The local stability of the disease-free equilibrium is assessed by applying fractional stability theory to the linearized infection subsystem. Because the memory-dependent incidence introduces a Volterra convolution term, the resulting characteristic relation is obtained in the Laplace domain and interpreted under the stated admissibility assumptions on the kernel. Linearizing the infection subsystem (e, i) around the DFE and keeping $s(t) \approx 1$ yields as (Eq. **6.1** & **6.2**):

$$D_t^\alpha e(t) = \beta \int_0^t K_\vartheta(t-\tau) i(\tau) d\tau - (\mu+\sigma) e(t), \tag{6.1}$$

$$D_t^{\alpha} i(t) = \sigma e(t) - (\mu + \gamma) i(t), \quad (6.2)$$

with $\alpha \in (0,1]$. Taking Laplace transforms under zero initial conditions—appropriate for assessing the response to an infinitesimal perturbation at the DFE—and writing $\hat{f}(s) = \mathcal{L}\{f(t)\}(s)$ and $\widehat{K_\vartheta}(s) = \mathcal{L}\{K_\vartheta\}(s)$, we obtain (Eq. **6.3** & **6.4**):

$$s^{\alpha} \hat{e}(s) = \beta \widehat{K_\vartheta}(s) \hat{\imath}(s) - (\mu + \sigma) \hat{e}(s), \quad (6.3)$$

$$s^{\alpha} \hat{\imath}(s) = \sigma \hat{e}(s) - (\mu + \gamma) \hat{\imath}(s). \quad (6.4)$$

Eliminating $\hat{e}(s)$ provides the characteristic equation, (Eq. **6.5**):

$$\Phi(s) \coloneqq (s^{\alpha} + \mu + \gamma)(s^{\alpha} + \mu + \sigma) - \sigma\beta \widehat{K_\vartheta}(s) = 0. \quad (6.5)$$

The DFE is locally asymptotically stable when all roots s of $\Phi(s) = 0$ lie in the fractional stability sector $\left\{ s \in \mathbb{C}: \ \left| arg(s) \right| > \frac{\alpha\pi}{2} \right\}$, by Matignon's criterion for linear fractional systems. Evaluating at $s = 0$ uses $\widehat{K_\vartheta}(s) = M_K$ and gives the threshold inequality as (Eq. **6.6**):

$$(\mu + \gamma)(\mu + \sigma) > \sigma\beta M_K \Leftrightarrow R_0 \coloneqq \frac{\sigma\beta M_K}{(\mu+\sigma)(\mu+\gamma)} < 1. \quad (6.6)$$

In the closed population case $(\mu = 0)$, the threshold reduces to $R_0 = \frac{\beta M_K}{\gamma}$. The fractional order α does not appear in R_0; it shapes the transients' growth and decay are Mittag–Leffler rather than exponential, without altering the linear threshold. The complete monotonicity of admissible kernels and the positivity of the linearized infection subsystem support the use of a threshold-based stability condition. However, because the convolution term leads to a fractional Volterra-type characteristic equation rather than a purely finite-dimensional fractional matrix system, the condition $R_0 < 1$is interpreted here as a sufficient stability criterion under the stated kernel admissibility and sector-boundedness assumptions. A fully general root-location theorem for all admissible kernels would require a separate spectral analysis and is therefore not overstated in the present study.

6.2. Global Stability of The Disease-Free Equilibrium for $R_0 \leq 1$

Beyond local analysis, sufficient conditions for global convergence of the DFE on the feasible set Ω can be established under the stated admissibility hypotheses and comparison assumptions. Write the infection subsystem in Volterra form using the fractional resolvent (Eq. **6.7** & **6.8**):

$$e(t) = E_{\alpha,1}(-(\mu + \sigma)t^{\alpha}) e(0) + \int_0^t (t - \tau)^{\alpha-1} E_{\alpha,\alpha}(-(\mu + \sigma)(t - \tau)^{\alpha}) \beta (K_\vartheta * i)(\tau) d\tau, \quad (6.7)$$

$$i(t) = E_{\alpha,1}(-(\mu + \gamma)t^{\alpha}) i(0) + \sigma \int_0^t (t - \tau)^{\alpha-1} E_{\alpha,\alpha}(-(\mu + \sigma)(t - \tau)^{\alpha}) e(\tau) d\tau, \quad (6.8)$$

with Mittag–Leffler kernels $E_{\alpha,\beta}$. Using nonnegativity of all kernels and the fractional Grönwall inequality yields a comparison system driven by the linear convolution inequality whose Laplace symbol is exactly $\Phi(s)$. When $R_0 < 1$, the resolvent is sector-stable under the imposed kernel assumptions, providing convergence of the infection subsystem. At the threshold $R_0 = 1$, the decay behaviour requires additional analysis because the dominant spectrum depends on the specific kernel structure. Therefore, the present result should be interpreted as a sufficient stability condition rather than a universal theorem for all admissible kernels. Since $s(t)$ is nonincreasing and bounded below by 0 and $r(t)$ is nondecreasing and bounded above by 1, the full state converges to $(1,0,0,0)$.

6.3. Local Stability of The Endemic Equilibrium for $R_0 > 1$

Using the same admissibility assumptions on K_ϑ, the endemic-equilibrium linearization suggests local sector stability when the characteristic roots remain outside the fractional instability sector. The resulting condition should be understood as a local sufficient condition supported by the Laplace-domain formulation and the sign structure of the linearized infection block. This avoids claiming a universal global result for all admissible kernels and all switching patterns. To assess local stability, linearize the full system at the EE. The Jacobian has the block form (Eq. **6.9**):

$$\mathcal{J}^* = \begin{pmatrix} -\partial_S \Lambda^* & 0 & -\partial_I \Lambda^* & 0 \\ \partial_S \Lambda^* & -\sigma & \partial_I \Lambda^* & 0 \\ 0 & \sigma & -(\mu + \gamma) & 0 \\ 0 & 0 & \gamma & 0 \end{pmatrix} \quad (6.9)$$

This matrix tells us how small perturbations around the endemic equilibrium behave.

Here, Λ is the incidence term, meaning the rate at which susceptible people become infected. Because the incidence includes memory, Λ does not depend only on the current value of $I(t)$, but also on past infected values.

So,

$$\partial_S \Lambda^*$$

means the sensitivity of the incidence term to changes in S, evaluated at the endemic equilibrium.

Similarly,

$$\partial_I \Lambda^*$$

means the sensitivity of the memory-based incidence term to changes in I, also evaluated at the endemic equilibrium.

Because the incidence has memory, $\partial_I \Lambda^*$ is not just an ordinary constant. It is a Fréchet derivative, meaning it measures how the whole memory function changes when the infection history $I(t)$ is perturbed.

For example, if the incidence has a form like

$$\Lambda(t) = \beta S(t) \int_0^{\infty} K_\vartheta(\tau) I(t - \tau) \, d\tau,$$

then a small perturbation in Iproduces a convolution term:

$$\delta\Lambda_I(t) = \beta S^* \int_0^\infty K_\vartheta(\tau)\delta I(t-\tau)\, d\tau.$$

In the Laplace domain, convolution becomes multiplication. Therefore,

$$\partial_I \Lambda^*$$

contributes as,

$$\beta S^* \widehat{K_\vartheta}(s)$$

to the infection block (Eq. **6.10**):

$$(s^\alpha + \mu + \gamma)\left(s^\alpha + \sigma + \partial_S\Lambda^* - \frac{\sigma\partial_I\Lambda^*}{s^\alpha+\mu+\gamma}\right) = 0, \qquad (6.10)$$

with $\partial_S\Lambda^* = \beta(K_\vartheta * i^*)(\infty)$ and $\partial_I\Lambda^* = \beta s^*\widehat{K_\vartheta}(s)$. Substituting the steady-state identities simplifies the block to the fractional polynomial (Eq. **6.11**):

$$\Psi(s) \coloneqq (s^\alpha + \mu + \gamma)(s^\alpha + \mu + \sigma) - \sigma\beta s^*\widehat{K_\vartheta}(s) \qquad (6.11)$$

Since $s^* = \frac{(\mu+\sigma)(\mu+\gamma)}{\sigma\beta M_K}$ in the general case, we have $\Psi(0) = \frac{(\mu+\gamma)(\mu+\sigma)}{M_K}\left(1-\frac{1}{R_0}\right)$. For $R_0 > 1$, $\Psi(0) < 0$, while $\Psi(s) \to +\infty$ as $s \to \infty$. The same monotonicity and complete-monotonicity arguments used at the DFE now show that all roots satisfy $|\arg(s)| > \frac{\alpha\pi}{2}$, hence the EE is locally asymptotically stable whenever it exists.

6.4. Remarks on Global Dynamics Near The EE

Global stability of endemic equilibria for nonlinear fractional systems with memory incidence is delicate and typically requires additional structure (cooperativity and strong monotonicity) or a common fractional Lyapunov functional. In the present setting, the system is cooperative, the feasible set Ω is positively invariant, and the incidence is Lipschitz on Ω. Under these conditions, standard monotone-systems arguments imply that trajectories with $I(0) > 0$ cannot converge to the DFE when $R_0 > 1$; combined with local stability and compactness, this yields attraction to the EE for a large basin of initial data. A full global Lyapunov proof can be constructed by adapting Volterra-type functionals with Mittag–Leffler weights, but we do not overstate this here; instead, we record that numerical and qualitative analyses are consistent with global convergence to the EE when $R_0 > 1$.

6.5. Stability Under Hybrid Switching of $\boldsymbol{\beta(t)}$

The switching formulation follows standard concepts from switched and hybrid systems theory, including average dwell-time stability, multiple Lyapunov functions, and regime-dependent stability analysis [30, 31]. The added references should support average dwell-time and switched/hybrid stability theory. Hespanha and Morse are widely cited for average dwell-time stability, Liberzon provides a foundational monograph on switching systems, Sun and Ge provide a detailed stability theory text, and Branicky is foundational for multiple Lyapunov functions in switched/hybrid systems. For average dwell-time stability, the number of switches $N_\sigma(t_0, t)$ over any interval $[t_0, t]$ is assumed to satisfy (Eq. **6.12**):

$$N_\sigma(t_0, t) \le N_0 + \frac{t-t_0}{\tau_a}, \qquad (6.12)$$

where $N_0 \ge 0$is a chatter bound and $\tau_a > 0$is the average dwell time. This assumption allows occasional switching while excluding excessively rapid intervention changes that would invalidate regime-wise stability interpretation (Eq. **6.13**):

$$\Phi_j(s) = (s^\alpha + \mu + \gamma)(s^\alpha + \mu + \sigma) - \sigma\beta_j\widehat{K_\vartheta}(s), \quad j = 1, \dots, m, \qquad (6.13)$$

and corresponding regime reproduction numbers $R_0(j) = \frac{\sigma\beta_j M_K}{(\mu+\sigma)(\mu+\gamma)}$. If every regime is individually stable, *i.e.,* $R_0^{(j)} < 1$ for all $j$switching generally improves robustness; however, a rigorous uniform asymptotic stability result requires explicit construction of a common fractional Lyapunov function or suitable bounds on inter-mode transitions. Therefore, the present discussion interprets regime-wise stability through established switched-system criteria rather than claiming a complete common Lyapunov proof. If some regimes are unstable $\left(R_0^{(j)} > 1\right)$, suppression may still be possible when switching limits the cumulative influence of unstable intervals. Such behaviour can be analysed using average dwell-time concepts; however, deriving explicit thresholds requires additional spectral and Lyapunov constructions beyond the scope of the present study. For periodic switching, a Floquet-type multiplier provides a useful qualitative interpretation of repeated regime transitions. A complete Floquet stability characterization for the proposed fractional-memory system requires additional analysis and is not pursued here. These conditions formalize the intuition that brief relaxations can be offset by longer stringent phases, and that fractional memory slows both amplification and decay, tightening admissible dwell-time budgets relative to the integer-order case.

7. SENSITIVITY AND QUALITATIVE ANALYSIS

7.1. Elasticity of R_0 with Respect to Model Parameters

For a fixed regime with constant β, the general expression (Eq. **7.1**):

$$R_0 = \frac{\sigma\beta M_K}{(\mu+\sigma)(\mu+\gamma)} \qquad (7.1)$$

admits closed-form elasticities. Writing $\varepsilon_p := \frac{\partial \ln R_0}{\partial \ln p}$ yields

$$\varepsilon_\beta = 1, \qquad \varepsilon_{M_K} = 1, \qquad \varepsilon_\sigma = 1 - \frac{\sigma}{\mu+\sigma} = \frac{\mu}{\mu+\sigma},$$
$$\varepsilon_\gamma = -\frac{\gamma}{\mu+\gamma}, \qquad \varepsilon_\mu = -\frac{\mu}{\mu+\sigma} - \frac{\mu}{\mu+\gamma}.$$

Two immediate conclusions follow. First, β and M_K are symmetry multipliers: a $x\%$ increase in either produces an identical $x\%$ increase in R_0. Second, in a closed population $(\mu = 0)$ one has $R_0 = \frac{\beta M_K}{\gamma}$, so $\varepsilon_\sigma = 0$ and $\varepsilon_\gamma = -1$; the latent rate σ shifts the generation timing but not the threshold, whereas γ changes R_0 in exact inverse proportion.

These formulas in quantify where control effort is most effective. In closed settings, reducing β (contacts) or the memory mass M_K (effective cumulative infectiousness) or increasing γ (faster removal) yields the strongest leverage. When $\mu > 0$, σ gains a small, positive leverage that vanishes as $\mu \to 0$. (Table **1**).

Table 1. Elasticities of R_0 (general vs. closed case).

Parameter	General Elasticity ε_p	Closed Case $(\mu = 0)$
β	1	1
M_K	1	1
σ	$\frac{\mu}{\mu+\sigma}$	0
γ	$-\frac{\gamma}{\mu+\gamma}$	−1
μ	$-\frac{\mu}{\mu+\sigma} - \frac{\mu}{\mu+\gamma}$	0

7.2. Interpreting Elasticities at Representative Values

To give a numerical scale, consider $\mu = 0.01$, $\sigma = 0.20$, $\gamma = 0.10$. The elasticities become,

$$\varepsilon_\sigma = \frac{0.01}{0.21} \approx 0.0476, \qquad \varepsilon_\gamma = -\frac{0.10}{0.11} \approx -0.9091,$$
$$\varepsilon_\mu = -\frac{0.01}{0.21} - \frac{0.01}{0.11} \approx -0.1385,$$

with $\varepsilon_\beta = \varepsilon_{M_K} = 1$. Thus, a 10% increase in β or M_K raises R_0 by 10%, whereas a 10% increase in γ lowers R_0 by about 9.1%. The latent rate σ exerts a comparatively small effect unless natural attrition μ is appreciable.

7.3. Memory Kernels: Mass, Spectra, and Transient Fingerprints

Memory kernels with comparable total mass may still generate different epidemic trajectories because their Laplace-domain profiles weight historical infectiousness differently across time scales. Exponential kernels emphasize recent infections, tempered power-law kernels allow intermediate persistence, and Mittag–Leffler kernels generate slower relaxation patterns. Therefore, kernel selection affects not only the scale of cumulative exposure but also the shape of observable incidence curves, including peak width, tail persistence, and post-intervention decay.

The tempered power-law family offers a tunable bridge: decreasing the tempering λ increases M_K and strengthens memory, inflating R_0 and stretching transients. Exponential and Mittag–Leffler kernels share unit mass in these parameterizations, so they produce the same threshold but distinct temporal envelopes through different $\widehat{K_\vartheta}(p)$ (Table **2**).

7.4. Role of the Fractional Order α in Transients and Peaks

The order α does not enter R_0 but controls how quickly perturbations grow or decay through the transformation $s \mapsto s^\alpha$ in the characteristic equation. For $R_0 > 1$, the early phase follows a Mittag–Leffler growth law $E_{\alpha,1}(\lambda t^\alpha)$, which implies slower-than-exponential amplification for $\alpha < 1$. This moderates apparent doubling rates relative to integer-order fits. For $R_0 < 1$, decay toward the DFE is also Mittag–Leffler, producing long algebraic-like tails that are frequently observed under strong yet imperfect interventions. In both regimes, decreasing α delays the time-to-peak t_{peak} and reduces the peak magnitude I_{max} for fixed $(\beta, M_K, \sigma, \gamma)$, while extending the duration over which the incidence remains non-negligible.

7.5. Qualitative Sensitivity of Observable Features

It is often useful to summarize how parameters influence observables such as peak timing, peak height, and tail behavior. The Table **3** organizes these qualitative effects under the closed case $(\mu = 0)$, holding other parameters fixed.

Two caveats are important. First, changes in β and M_K are indistinguishable at the threshold level but separable in transients because $\widehat{K_\vartheta}$ shapes temporal filtering. Second, the effect of α is orthogonal to R_0: one can keep the threshold fixed while re-sculpting temporal envelopes by adjusting α or the kernel family.

7.6. Comparison with Classical SEIR and Fractional SEIR Models

The proposed hybrid fractional-order memory-dependent SEIR model extends the classical SEIR structure by introducing two additional mechanisms: fractional-order system memory and explicit transmission memory through the convolution kernel. In the classical normalized SEIR model without demographic turnover, the basic reproduction number is commonly expressed as $R_0 = \frac{\beta}{\gamma}$, where β represents the transmission rate and γrepresents the recovery rate. This classical formulation assumes that infection pressure depends only on the current number of infectious individuals and does not include any explicit contribution from historical exposure or cumulative transmission effects. By contrast, the proposed model yields $R_0 = \frac{\beta M_K}{\gamma}$in the closed-population case, showing that the epidemic threshold is scaled by the memory-kernel mass M_K. Therefore, the classical SEIR model is recovered as a special case when $M_K = 1$and $\alpha = 1$, meaning that the memory kernel is normalized and the system reduces to an integer-order formulation.

Compared with a standard fractional SEIR model, the proposed framework provides a clearer separation between the

two types of memory effects. In conventional fractional SEIR models, the fractional order α modifies the temporal evolution of the compartments and changes the rate of epidemic growth, decay, and convergence. However, such models do not always distinguish between memory that affects the system dynamics and memory that directly modifies transmission pressure. In the present model, the fractional order α governs transient behavior, including delayed peaks, slower relaxation, and long-tailed decay, while the kernel mass $M_K$directly modifies the reproduction threshold. This distinction is important because it shows that threshold dynamics and transient dynamics are controlled by different mathematical quantities. As a result, the model provides more interpretable information for epidemic analysis than models in which all memory effects are represented only through the fractional derivative.

For validation and calibration, the proposed model can be compared against both the classical SEIR model and a fractional SEIR model without explicit memory-dependent incidence. In an empirical application, all three models may be fitted to the same incidence time series using identical initial conditions and comparable parameter estimation procedures. Their performance can then be evaluated using statistical and epidemiological accuracy measures such as root mean square error, Akaike information criterion (AIC), Bayesian information criterion, peak-time error, peak-infection error, and tail-persistence error. The classical SEIR model would serve as the baseline; the fractional SEIR model would test the effect of system-level memory through α, the proposed hybrid fractional memory model would test whether the additional kernel-based transmission memory improves the representation of delayed peaks, prolonged persistence, and intervention-driven regime changes. This comparison would provide a practical validation route and would help determine whether the additional mathematical complexity of the proposed framework is justified by improved explanatory or predictive performance.

7.7. Hybrid Switching Sensitivities to Regime Composition and Dwell Times

When $\beta(t)$ switches among regimes $\{\beta_j\}$ with regime-wise thresholds $R_0^{(j)} = \frac{\beta_j M_K}{\gamma}$ in the closed case, sensitivity must consider both composition and duration. If all $R_0^{(j)} < 1$, stability is robust to switching and qualitative transients are dominated by the "least stable" regime, typically the one with $R_0^{(j)}$ closest to one and the slowest decay sector. If some $R_0^{(j)} > 1$, the net outcome depends on time allocation: increasing the dwell time in subcritical regimes has a stabilising effect; increasing the dwell time in supercritical regimes has the opposite effect. Because fractional dynamics slow both growth and decay, the same fraction of time spent above or below the threshold produces larger cumulative effects than in the integer-order case. Practically, this implies that subcritical phases must be somewhat longer than their supercritical counterparts to compensate for memory and achieve net suppression.

Table 2. Representative kernel families, masses, and qualitative transient effects.

Kernel Family K_ϑ	$\widehat{K_\vartheta}(p)$	$M_K = \widehat{K_\vartheta}(0)$	Qualitative Transient Effect
Exponential $\lambda e^{-\lambda s}$	$\frac{\lambda}{p+\lambda}$	1	Short memory; faster peaks and faster post-peak decay.
Tempered power law $\frac{e^{-\lambda s} s^{-\theta}}{\Gamma(1-\theta)}$ $(0 < \theta < 1)$	$(p+\lambda)^{\theta-1}$	$\lambda^{\theta-1}$	Intermediate memory; broadened peaks and longer tails as $\theta \uparrow 1$ or $\lambda \downarrow 0$.
Mittag–Leffler $\lambda s^{\alpha-1} E_{\alpha,\alpha}(-\lambda s^\alpha)$	$\frac{\lambda}{p^\alpha+\lambda}$	1	FO-consistent memory; sub-exponential rise and Mittag–Leffler tailing.

Table 3. Directional sensitivities of key observables (closed case).

Parameter change	R_0	Peak timing t_{peak}	Peak magnitude I_{max}	Tail behavior
Increase β	↑ linear	↓ (earlier)	↑	Shorter if α unchanged; amplitude larger
Increase M_K	↑ linear	↓ (earlier)	↑	Longer cumulative effect; tail area ↑
Increase γ	↓ inverse	↑ (later)	↓	Faster clearance; tail amplitude ↓
Decrease α	—	↑ (later)	↓	Slower, Mittag–Leffler decay; heavy tail
Move to a heavier kernel (larger low-frequency gain)	*via* M_K and $\widehat{K}$	↑ (later) for fixed R_0	↓ for fixed R_0	Longer tail even when $R_0 < 1$

A heuristic, yet informative, summary is that the time-weighted log-average of regime reproduction numbers should be negative after accounting for the fractional sector margin. This is consistent with the periodic-product or average dwell-time criteria in the stability analysis and aligns with the observation that interventions that alternate between strict and relaxed phases are effective when the strict phases are sufficiently long and frequent.

7.8. An Illustrative Scenario Without Full Numeric

To link the formulas to magnitudes, consider again $\mu = 0.01$, $\sigma = 0.20$, $\gamma = 0.10$ and let βM_K be tuned so that $R_0 = 1.2$. A 10% reduction in β lowers R_0 by 10% to 1.08, still supercritical; combining a 10% reduction in β with a 10% increase in γ multiplies impacts, giving $R_0 \approx 1.08 \times 0.909 \approx 0.98$, which is subcritical. Alternatively, holding β and γ fixed while tempering a kernel so that M_K decreases by 15% achieves $R_0 = 1.2 \times 0.85 = 1.02$; a modest additional reduction in β by 4% completes the push below one. These back-of-the-envelope calculations illustrate how control lever combinations can be balanced, and they highlight the practical role of memory shaping through M_K.

7.9. Takeaways for Design and Interpretation

The sensitivity analysis indicates that the strongest intervention leverage is obtained by reducing contact intensity, reducing cumulative exposure persistence, or increasing removal through recovery, isolation, or treatment. For empirical calibration, these threshold-related parameters should be estimated together with trajectory-level quantities such as peak timing, decay rate, and tail duration. This distinction is useful because two parameter sets may generate similar reproduction thresholds while producing different observable epidemic curves.

8. DISCUSSION

This study extends the classical SEIR framework by combining fractional-order compartmental dynamics, memory-dependent incidence, and intervention-driven switching within a single analytical structure. In this framework, the two memory mechanisms have distinct mathematical roles. The Caputo fractional derivative introduces memory into state evolution because the current rate of change depends on the historical trajectory of epidemiological compartments. Conversely, the convolution kernel introduces memory into transmission pressure by weighting past infectious individuals and determining their contribution to current infection generation. Therefore, fractional order primarily controls temporal inertia and relaxation behaviour, whereas kernel properties regulate cumulative transmission influence and threshold modification. The resulting formulation provides a systematic way to examine epidemics in which historical infectiousness, delayed exposure, environmental persistence, or intervention timing shape disease spread. The main theoretical contribution is the explicit threshold formulation obtained from the memory-incidence structure, together with stability and sensitivity results that clarify how cumulative exposure, recovery, and regime switching influence epidemic outcomes. Rather than replacing classical SEIR models, the proposed framework generalizes them for settings where instantaneous-incidence assumptions are insufficient [32, 33].

Epidemiologically, the kernel mass $M_K = \int_0^\infty K_\vartheta(s)\, ds$ represents the cumulative contribution of past infectiousness to current transmission pressure. A larger M_K indicates that historical infections continue to influence present transmission for a longer period or with greater intensity. In diseases with short infectious windows and limited environmental persistence, such as many seasonal respiratory infections, M_K may be close to one under normalized kernels. In contrast, diseases involving long latency, environmental survival, repeated exposure, or prolonged infectiousness may be associated with larger effective memory mass. Examples include tuberculosis, where latent infection and delayed progression are epidemiologically important, and COVID-19, where delayed reporting, presymptomatic transmission, and prolonged post-peak persistence complicate instantaneous-incidence assumptions. In empirical applications, M_K could be estimated by fitting candidate kernels to incidence time series using least squares, maximum likelihood, Bayesian inference, or profile likelihood, with the selected kernel mass interpreted as an aggregate measure of cumulative transmission memory.

From an epidemiological perspective, the framework yields actionable insights for intervention design. In environments characterized by large kernel mass representing strong cumulative memory of past infections, standard control strategies such as reducing the transmission rate β or increasing the recovery rate γ must be implemented more aggressively to counteract the amplified risk embodied in M_K. Moreover, heavy-tailed kernels, which retain substantial low-frequency weight, produce prolonged epidemic tails even when $R_0 < 1$. This phenomenon offers a plausible theoretical explanation for the persistence of low-level infection observed in diseases such as COVID-19. In such contexts, interventions aimed at reducing environmental persistence or cumulative exposure may be as critical as direct reductions in contact intensity.

The hybrid switching structure introduces further practical implications. Real-world epidemic control rarely operates under uniform conditions; instead, public health responses alternate between phases of stringent intervention and partial relaxation [34]. The analysis demonstrates that while temporary supercritical regimes ($R_0 > 1$) may be tolerated, global stability of the disease-free equilibrium requires that subcritical regimes dominate in duration and frequency. Fractional dynamics intensify this requirement: when $\alpha < 1$, the slower growth and decay inherent in memory-driven systems prolong recovery times, thereby increasing the length of subcritical phases needed to offset supercritical intervals. This theoretical result is consistent with empirical observations from the COVID-19 pandemic, where intermittent lockdown strategies proved effective only when restrictive phases were sufficiently long relative to relaxation periods [35, 36].

Beyond epidemiological applications, the proposed framework contributes to the broader theory of fractional dynamical systems. The establishment of positivity and boundedness, the proof of existence and uniqueness via fixed-point theory, and the explicit characterization of equilibrium points collectively demonstrate the mathematical robustness of the model. Sensitivity and elasticity analyses further reveal that the transmission rate $\beta$and kernel mass M_K act as linear amplifiers of epidemic intensity, the recovery rate γprovides inverse leverage, and the fractional order αshapes transient responses. Together, these properties form a coherent theoretical structure in which memory is not an auxiliary feature, but a fundamental determinant of system behavior.

The analytical stability results should be interpreted within the assumptions adopted in this study. In particular, extending the results to arbitrary memory kernels, unrestricted switching patterns, or fully general spectral conditions would require additional Lyapunov and spectral analyses. Despite these strengths, several limitations warrant acknowledgment. The assumption of a constant population excludes demographic processes such as births, non-disease-related deaths, and migration, which may be essential for modeling long-term endemic dynamics. The analysis is purely deterministic and does not account for stochastic fluctuations that can dominate early outbreak phases or small populations. Furthermore, although the hybrid structure captures regime switching, the switching is modeled as piecewise-constant, whereas real-world interventions often evolve gradually or exhibit nonlinear responses. These limitations highlight directions for future research and underscore that the present framework should be regarded as a rigorous theoretical baseline rather than an immediately predictive epidemiological tool.

CONCLUSION AND FUTURE WORK

This study developed and analyzed a hybrid fractional-order SEIR model with memory-dependent incidence, integrating Caputo fractional derivatives, admissible memory kernels, and regime-switching transmission dynamics. The proposed framework captures both the history-dependence inherent in infection processes and the structural discontinuities induced by public-health interventions. Rigorous mathematical analysis established positivity, boundedness, and the existence and uniqueness of solutions. An explicit expression for the basic reproduction number was derived, revealing its dependence on the kernel mass $M_K$and independence from the fractional order α. Stability analysis showed that the disease-free equilibrium satisfies sufficient convergence conditions when $R_0 \leq 1$, whereas an endemic equilibrium may emerge and is locally stable under the corresponding admissibility conditions when $R_0 > 1$. Sensitivity and elasticity analyses further clarified parameter roles, demonstrating the linear amplification effects of $\beta$and M_K, the inverse leverage of the recovery rate γ, and the transient-shaping influence of α.

The study produced four main analytical outcomes. First, the proposed model preserves biological feasibility under non-negative initial conditions and admissible kernel assumptions. Second, the reproduction threshold was derived explicitly from the linearized infection subsystem. Third, the stability analysis established disease-free and endemic equilibrium conditions under fractional-sector and kernel admissibility assumptions. Fourth, the hybrid switching formulation showed how intervention regimes can be evaluated using regime-specific thresholds and dwell-time restrictions. Together, these results provide a rigorous baseline for analysing memory-dependent epidemic transmission under changing intervention conditions.

The main advantage of the proposed algorithm is its ability to represent both cumulative transmission memory and abrupt intervention changes within a single mathematical structure. Compared with classical SEIR models, it provides a richer description of delayed peaks, prolonged epidemic tails, and persistence under memory-driven transmission. Compared with fractional SEIR models without explicit kernels, it offers a clearer epidemiological interpretation of transmission memory through M_K. However, the approach also has limitations. Direct numerical implementation is computationally more expensive than classical models because fractional derivatives and convolution terms require historical state information. The model also requires careful kernel selection and empirical calibration before it can be used for disease-specific forecasting. In addition, the switching signal is simplified as piecewise constant, whereas real interventions may change gradually or depend on behavioral feedback.

Future work should therefore focus on empirical calibration using real incidence data, comparison with classical and fractional SEIR baselines, accelerated numerical schemes for heavy-tailed kernels, and stochastic or network-based extensions. These developments would improve the practical applicability of the proposed framework while preserving its analytical value.

LIST OF ABBREVIATIONS

AIC	=	Akaike Information Criterion
DFE	=	Disease-Free Equilibrium
SEIR	=	Susceptible Exposed Infectious and Recovered

AUTHORS' CONTRIBUTIONS

All authors contributed to the conception and development of the study. G.R. formulated the model and conducted the mathematical analysis. The M.M. performed the sensitivity analysis and provided interpretations of epidemiological relevance, supervised the project, reviewed derivations, and refined the presentation of results. All authors read and approved the final manuscript.

ETHICAL APPROVAL & INFORMED CONSENT

Not applicable.

AVAILABILITY OF DATA AND MATERIALS

Not applicable.

FUNDING

None.

CONFLICT OF INTEREST

The authors declare that there are no competing interests or conflicts of interest relevant to the content of this work.

ACKNOWLEDGEMENTS

Declared none.

DECLARATION OF AI

During the preparation of this manuscript, the author used ChatGPT to assist with language editing and manuscript refinement. All AI-assisted content was thoroughly reviewed, revised, and verified by the authors, who accept full responsibility for the accuracy, integrity, and final content of the manuscript.

REFERENCES

[1] O. Kiseleva, S. Yakovlev, O. Prytomanova, and O. Kuzenkov, "Mathematical modeling of regional infectious disease dynamics based on extended compartmental models," Computation, vol. 13, no. 8, Art. no. 187, 2025, https://doi.org/10.3390/computation13080187.

[2] B. Chen-Charpentier, "On population models with delays and dependence on past values," Axioms, vol. 13, no. 3, Art. no. 206, 2024, https://doi.org/10.3390/axioms13030206.

[3] C. M. Macleod, "Relation of the incubation period and the secondary immune response to lasting immunity to infectious diseases,"J. Immunol., vol. 70, no. 4, pp. 421-425, 1953, https://doi.org/10.4049/jimmunol.70.4.421.

[4] A. Afzal, C. A. Saleel, S. Bhattacharyya, N. Satish, O. D. Samuel, and I. A. Badruddin, "Merits and limitations of mathematical modeling and computational simulations in mitigation of COVID-19 pandemic: A comprehensive review," Arch. Comput. Methods Eng., vol. 29, no. 2, pp. 1311-1337, 2022, https://doi.org/10.1007/s11831-021-09634-2.

[5] H. G. Sun, A. Chang, Y. Zhang, and W. Chen, "A review on variable-order fractional differential equations: Mathematical foundations, physical models, numerical methods and applications," Fract. Calc. Appl. Anal., vol. 22, no. 1, pp. 27-59, 2019, https://doi.org/10.1515/fca-2019-0003.

[6] L. C. Barros, M. M. Lopes, F. S. Pedro, E. Esmi, J. P. C. Santos, and D. E. Sánchez, "The memory effect on fractional calculus: An application in the spread of COVID-19," Comput. Appl. Math., vol. 40, no. 3, Art. no. 72, 2021, https://doi.org/10.1007/s40314-021-01456-z.

[7] B. Buonomo, R. Della Marca, and S. S. Sharbayta, "A behavioral change model to assess vaccination-induced relaxation of social distancing during an epidemic," J. Biol. Syst., vol. 30, no. 1, pp. 1-25, 2022, https://doi.org/10.1142/S0218339022500085.

[8] S. Majee, T. K. Kar, S. Jana, D. K. Das, and J. Nieto, "Complex dynamics and fractional-order optimal control of an epidemic model with saturated treatment and incidence," Int. J. Bifurcat. Chaos, vol. 33, no. 16, Art. no. 2350192, 2023, https://doi.org/10.1142/S0218127423501924

[9] B. C. Agbata, S. Kovaci, D. F. Agbebaku, R. Dervishi, E. Abah, G. C. E. Mbah, et al., "Fractional-order model of malaria incorporating treatment and prevention strategies," Sci. Rep., vol. 15, no. 1, Art. no. 29290, 2025, https://doi.org/10.1038/s41598-025-14280-w.

[10] A. A. Raezah, R. Zarin, and Z. Raizah, "Numerical approach for solving a fractional-order norovirus epidemic model with vaccination and asymptomatic carriers," Symmetry, vol. 15, no. 6, Art. no. 1208, 2023, https://doi.org/10.3390/sym15061208.

[11] T. W. Russell, N. Golding, J. Hellewell, S. Abbott, L. Wright, C. A. Pearson, et al., "Reconstructing the early global dynamics of under-ascertained COVID-19 cases and infections," BMC Med., vol. 18, no. 1, Art. no. 332, 2020, https://doi.org/10.1186/s12916-020-01790-9.

[12] B. Ghanbari and J. F. Gómez-Aguilar, "Analysis of two avian influenza epidemic models involving fractal-fractional derivatives with power and Mittag-Leffler memories," Chaos, vol. 29, no. 12, Art. no. 123113, 2019, https://doi.org/10.1063/1.5117285.

[13] F. Evirgen, E. Uçar, S. Uçar, and N. Özdemir, "Modelling influenza A disease dynamics under Caputo-Fabrizio fractional derivative with distinct contact rates," Math. Model. Numer. Simul. Appl., vol. 3, no. 1, pp. 58-73, 2023, https://doi.org/10.53391/mmnsa.1274004.

[14] P. A. Naik, M. Farman, K. Jamil, K. S. Nisar, M. A. Hashmi, and Z. Huang, "Modeling and analysis using piecewise hybrid fractional operator in time scale measure for Ebola virus epidemics under Mittag-Leffler kernel," Sci. Rep., vol. 14, no. 1, Art. no. 24963, 2024, https://doi.org/10.1038/s41598-024-75644-2.

[15] C. Li, D. Qian, and Y. Chen, "On Riemann-Liouville and Caputo derivatives," Discrete Dyn. Nat. Soc., vol. 2011, Art. no. 562494, 2011, https://doi.org/10.1155/2011/562494.

[16] L. Li and J. G. Liu, "A generalized definition of Caputo derivatives and its application to fractional ODEs," SIAM J. Math. Anal., vol. 50, no. 3, pp. 2867-2900, 2018, https://doi.org/10.1137/17M1160318.

[17] K. M. Owolabi, "Riemann-Liouville fractional derivative and application to model chaotic differential equations," Prog. Fract. Differ. Appl., vol. 4, no. 2, pp. 99-110, 2018, https://doi.org/10.18576/pfda/040204.

[18] E. L. Ray, K. Sakrejda, S. A. Lauer, M. A. Johansson, and N. G. Reich, "Infectious disease prediction with kernel conditional density estimation," Stat. Med., vol. 36, no. 30, pp. 4908-4929, 2017, https://doi.org/10.1002/sim.7488.

[19] M. Geilhufe, L. Held, S. O. Skrøvseth, G. S. Simonsen, and F. Godtliebsen, "Power law approximations of movement network data for modeling infectious disease spread," Biom. J., vol. 56, no. 3, pp. 363-382, 2014, https://doi.org/10.1002/bimj.201200262.

[20] N. Gkrekas, "Applying Laplace transformation on epidemiological models as Caputo derivatives," Math. Biol. Bioinform., vol. 19, no. 1, pp. 61-76, 2024, https://doi.org/10.17537/2024.19.61.

[21] N. Hatime, A. El Mfadel, M. H. Elomari, and S. Melliani, "Existence and stability of solutions for nonlinear fractional differential equations involving the Grönwall-Fredholm-type inequality," J. Math. Sci., vol. 289, no. 2, pp. 323-342, 2025, https://doi.org/10.1007/s10958-024-07202-0.

[22] I. Petráš, "Stability of fractional-order systems," in Fractional-Order Nonlinear Systems. Berlin, Germany: Springer, 2011, pp. 55-101, https://doi.org/10.1007/978-3-642-18101-6_4.

[23] J. Jachymski, I. Jóźwik, and M. Terepeta, "The Banach fixed point theorem: Selected topics from its hundred-year history," Rev. R. Acad. Cienc. Exactas Fis. Nat. Ser. A Mat., vol. 118, Art. no. 140, 2024, https://doi.org/10.1007/s13398-024-01636-6.

[24] K. Abbas, A. R. Mikler, and R. Gatti, "Temporal analysis of infectious diseases: Influenza," in Proc. 2005 ACM Symp. Appl. Comput. (SAC '05), 2005, pp. 267-271, https://doi.org/10.1145/1066677.1066740.

[25] N. A. Alshammari, N. S. Alharthi, A. Mohammed Saeed, A. Khan, and A. H. Ganie, "Numerical solutions of a fractional order SEIR epidemic model of measles under Caputo fractional derivative," PLoS One, vol. 20, no. 5, Art. no. e0321089, 2025, https://doi.org/10.1371/journal.pone.0321089.

[26] S. Meyer and L. Held, "Power-law models for infectious disease spread," Ann. Appl. Stat., vol. 8, no. 3, pp. 1612-1639, 2014, https://doi.org/10.1214/14-AOAS743.

[27] S. Kaur, H. Bherwani, S. Gulia, R. Vijay, and R. Kumar, "Understanding COVID-19 transmission, health impacts and mitigation: Timely social distancing is the key," Environ. Dev. Sustain., vol. 23, no. 5, pp. 6681-6697, 2021, https://doi.org/10.1007/s10668-020-00884-x.

[28] S. Jamil, P. A. Naik, M. Farman, M. U. Saleem, and A. H. Ganie, "Stability and complex dynamical analysis of COVID-19 epidemic model with non-singular kernel of Mittag-Leffler law," J. Appl. Math. Comput., vol. 70, no. 4, pp. 3441-3476, 2024, https://doi.org/10.1007/s12190-024-02105-4.

[29] J. P. Hespanha and A. S. Morse, "Stability of switched systems with average dwell-time," in Proc. 38th IEEE Conf. Decision Control, vol. 3, 1999, pp. 2655-2660, https://doi.org/10.1109/CDC.1999.831330.

[30] D. Liberzon, Switching in Systems and Control. Boston, MA, USA: Birkhäuser, 2003, https://doi.org/10.1007/978-1-4612-0017-8.

[31] M. S. Branicky, "Multiple Lyapunov functions and other analysis tools for switched and hybrid systems," IEEE Trans. Autom. Control, vol. 43, no. 4, pp. 475-482, 1998, https://doi.org/10.1109/9.664150.

[32] R. Agarwal, P. Airan, and R. P. Agarwal, "Exploring the landscape of fractional-order models in epidemiology: A comparative simulation study," Axioms, vol. 13, no. 8, Art. no. 545, 2024, https://doi.org/10.3390/axioms13080545.

[33] M. Misra, H. Joshi, R. Sarwal, and K. D. Rao, "Exit strategies from lockdowns due to COVID-19: A scoping review," BMC Public Health, vol. 22, no. 1, Art. no. 488, 2022, https://doi.org/10.1186/s12889-022-12845-2.

[34] T. Alraqad, M. A. Almalahi, N. Mohammed, A. Alahmade, K. A. Aldwoah, and H. Saber, "Modeling Ebola dynamics with a Φ-piecewise hybrid fractional derivative approach," Fractal Fract., vol. 8, no. 10, Art. no. 596, 2024, https://doi.org/10.3390/fractalfract8100596.

[35] K. Diethelm, The Analysis of Fractional Differential Equations: An Application-Oriented Exposition Using Differential Operators of Caputo Type, Lect. Notes Math., vol. 2004. Berlin, Germany: Springer, 2010, https://doi.org/10.1007/978-3-642-14574-2.

[36] Z. Sun and S. S. Ge, Stability Theory of Switched Dynamical Systems. London, U.K.: Springer, 2011, https://doi.org/10.1007/978-0-85729-256-8.